FINITE ELEMENT MODELING OF THE ARCHING EFFECT IN RETAINING WALLS MADE OF SOIL MIX PANELS

Nicolas Denies, Belgian Building Research Institute, Geotechnical Division, Belgium, nde@bbri.be
Malek Allani, Belgian Building Research Institute, BBRI, Limelette, Belgium, mal@bbri.be
Noël Huybrechts, Belgian Building Research Institute & KU Leuven, Belgium, nh@bbri.be
Jean-Cédric Kouamé, Franki Foundations Belgium SA, Saintes, Belgium, Jean-Cedric.Kouame@ffgb.be
Grégory Laurent, Franki Foundations Belgium SA, Saintes, Belgium, Gregory.Laurent@ffgb.be
Tim Eggermont, Franki Foundations Belgium SA, Saintes, Belgium, Tim.Eggermont@ffgb.be
Maurice Bottiau, Franki Foundations Belgium SA, Saintes, Belgium, mail@ffgb.be

ABSTRACT

Since 2000, the Deep Mixing is more and more applied for the construction of retaining structures. The working principle of a soil mix wall with a retaining function is mainly based on the development of an arching effect through the soil mix material to transmit the earth and water pressures, acting behind the retaining wall, to the steel beams inserted in the fresh soil mix material during execution. Example calculations of the arching effect in Plaxis 2D have recently been provided for soil mix rectangular panels in the BBRI/SBRCURnet Handbook - Soil mix walls, referred as the handbook in the present paper. A 2D analysis had been made in finite element calculations to verify the pattern of the arching effect.
Based on a similar model, the authors analyze the development of such pressure arch in soil mix panels. The effect of the tensile resistance of the soil mix material is studied. The influences of the boundary conditions and the mesh refinement are also investigated. Finally, a comparison is made between the results of the numerical models and the analytical solutions proposed in the handbook for the structural verification of the soil mix walls with a retaining function according to the Eurocodes, the building codes for Europe.

Keywords: soil mix walls, retaining walls, CSM panels, FEM, arching effect, design

INTRODUCTION – CSM RETAINING WALLS AND FEM OF THE ARCHING EFFECT

In order to build a retaining wall for the realization of an excavation, soil mix panels can be placed next to each other, in a secant way (see Fig. 1). By overlapping the different panels, a continuous retaining wall is built. The wall is then horizontally stabilized with the help of bracing or anchoring systems. During execution, steel H or I-beams are generally installed in the fresh soil mix material to resist the shear forces and bending moments due to the pressure applying on the wall. The soil mix material mainly transmits the stresses due to this pressure to the steel beams by way of an arching effect developing in the soil mix due to the difference of stiffness between the steel and the soil mix material. Figure 2 illustrates the working principle of a soil mix wall with a retaining function. CSM panels present typical lengths ranging between 2.2 to 2.8 m, a thickness of 55 cm and common installation depths up to 20 m.
The present article focuses on the arching effect arising in soil mix panels when subjected to the pressure acting behind the retaining wall. In this study, a 2D FEM model, built with PLAXIS, is used. The effect of the tensile strength of the soil mix material is first investigated. The influences of the boundary conditions and the mesh refinement on the development of the pressure arch are also regarded. Finally, a comparison is made between the numerical results and the analytical solutions given in the handbook. In the simulations, the soil is not directly considered. Only a uniform pressure of 50 kPa (corresponding depth of about 5 m) is applied on the soil mix material which is modeled with an elasto-plastic behavior and a failure criterion type Mohr-Coulomb. We are working in plane strain configuration (no vertical deformation). The soil mix material can freely move in the direction of the pressure load, but the deformations and displacements are prevented in the lateral directions, at the model boundaries. The displacement of the steel beams is prevented with fixed points (black anchor lines in the figures). Table 1 presents the data, the geometry and the parameters of the model. For the initial simulations, a medium mesh is used without local refinement.

Fig. 1. Retaining wall made of secant reinforced CSM panels – construction site in Belgium

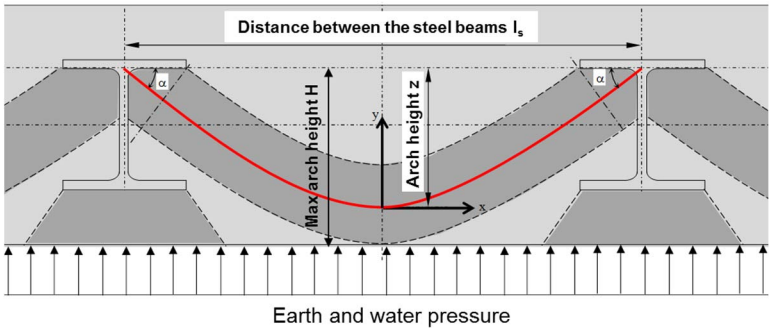

Fig. 2. Working principle of a soil mix retaining wall and illustration of the arching effect

PARAMETRIC STUDIES: TENSILE STRENGTH, BOUNDARIES AND MESH REFINEMENT

Figure 3 illustrates the pressure arch developing, between the steel beams, in the soil mix material. With the decrease of the tensile strength of the soil mix, the compression arch is more and more visible.
Table 2 presents the numerical results for the stresses developing inside the pressure arch in function of the characteristic value of the tensile strength, $f_{sm,tk}$, considered for the soil mix material. In this table, the stress values are compared for the same cross-sections, respectively given in Fig. 4, 5 and 6. The stress values indicated in Table 2 are the maximal stress values for the stress distributions (illustrated in Fig. 4, 5 and 6) developing along each determined cross-section. Regarding the stress pattern in the panel, illustrated in Fig. 7 and 8, the selection of the cross-section considered for the analyze will have an important influence on the stress values. The verification of the panel will therefore be realized based on the internal resultant forces developing inside the material in addition to the analysis of local stress distributions.
Regarding the stress values of Table 2, the **influence of the tensile strength** of the soil mix material is obvious. For the simulation with $f_{sm,tk}$ equal to 2.0 MPa, the compressive and tensile strengths of the soil mix material are nowhere reached when a uniform pressure of 50 kPa is applied on the wall. For the simulation with $f_{sm,tk}$ = 0.1 MPa, the tensile strength is reached only for the part of the soil mix material above the flange of the steel beams (see Fig. 9). Figure 9 highlights the plastic points developing in the soil mix material. The red points represent material points where the tensile strength is reached in the soil mix material. As this zone is very limited, the stress distribution in the wall is almost the same than in the simulation with $f_{sm,k}$ = 2.0 MPa for which no plastic point is observed. For the simulation with $f_{sm,tk}$ = 0 MPa, the zone affected by plastic points is more extensive (see Fig. 10). As a consequence, the maximal compression stress, observed in the middle of the arch, is almost doubled in comparison with the compression stresses obtained with $f_{sm,tk}$ = 2 or 0.1 MPa. In spite of the plastic points observed in the simulations for a $f_{sm,tk}$ of 0 and 0.1 MPa, no global failure or instability of the soil mix wall is observed. The decrease of the tensile strength still affects the stress distribution in the CSM panel.

Table 1. Data, geometry and parameters of the present model

Soil mix parameters	
Thickness (=height) of the CSM panel, h_{sm}	0.55 m
Characteristic value of the Unconfined Compressive Strength (UCS) of the soil mix material, $f_{sm,k}$	2.0 MPa
Modulus of elasticity, E_{sm} (with E_{sm} = 1000 $f_{sm,k}$ in first approximation as referred in the handbook)	2.0 GPa
Charcteristic value of the tensile strength of the soil mix material, $f_{sm,tk}$	Variable
Cohesion of the soil mix material, c'	1000 kPa
Internal friction angle of the soil mix material, ϕ'	0.1°
Steel beam parameters	
Type of steel beam	IPE 360
Modulus of elasticity of the steel	210 GPa
Height of the beam, h_a	360 mm
Thickness of the web, t_w	8.0 mm
Width of the flange, b_f	170.0 mm
Thickness of the flange, t_f	12.7 mm
Axis-to-axis distance between the steel beams, l_s	1.22 m
Cover of the beam (compressive and tensile sides): c_1 = c_2	9.5 cm

Table 2. Plaxis 2D calculation results obtained regarding the arching effect in the soil mix material

MODEL	**$f_{sm,tk}$ = 2 MPa**	**$f_{sm,tk}$ = 0.1 MPa**	**$f_{sm,tk}$ = 0 MPa**
Maximal† compressive stress at the base of the pressure arch (kPa)	76	76	135
Maximal† compressive stress in the middle of the pressure arch (kPa)	78	79	222
Maximal† shear stress in the pressure arch (kPa)	63	64	110

†Maximal stress value for the stress distribution developing along the determined cross-section (see Fig. 4, 5 and 6)

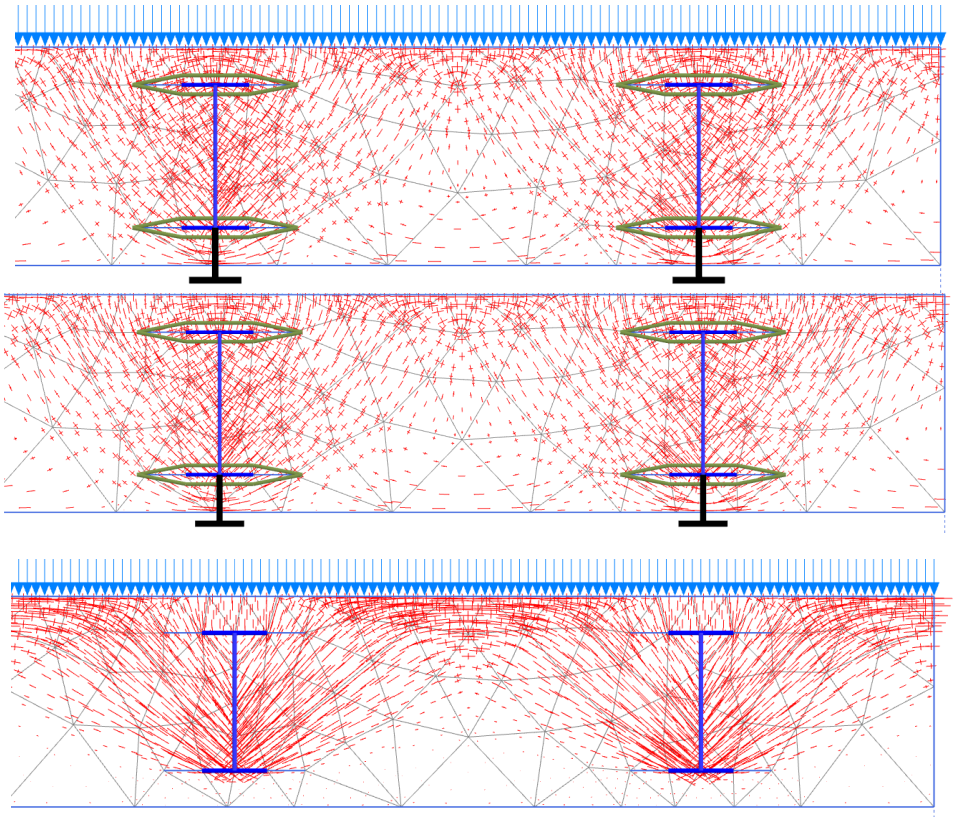

Fig. 3. Development of the arching effect in the soil mix material: total principal stresses (above: $f_{sm,tk}$ = 2 MPa, in the middle: $f_{sm,tk}$ = 0.1 MPa, below: $f_{sm,tk}$ = 0 MPa)

Fig. 4. Total normal stress distribution, σ_N, at the base of the pressure arch (for $f_{sm,tk}$ = 0.1 MPa)

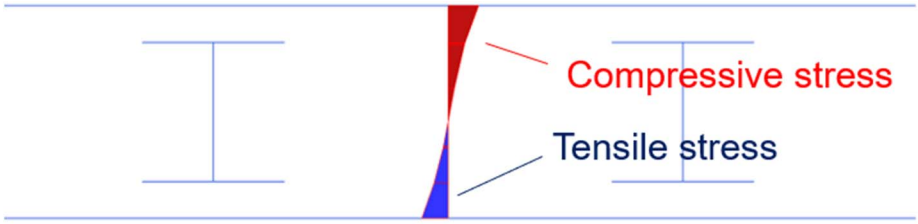

Fig. 5. Total normal stress distribution, σ_N, in the middle of the pressure arch ($f_{sm,tk}$ = 0.1 MPa)

Fig. 6. Shear stress distribution, τ_S, developing along the cross-section at the boundaries of the flanges of the steel beam (for $f_{sm,tk}$ = 0.1 MPa)

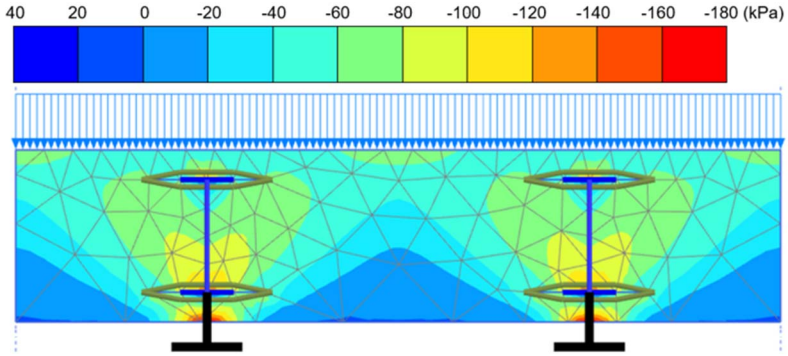

Fig. 7. Principal total stress, σ_1, in the pressure arch (with $f_{sm,tk}$ = 0.1 MPa)

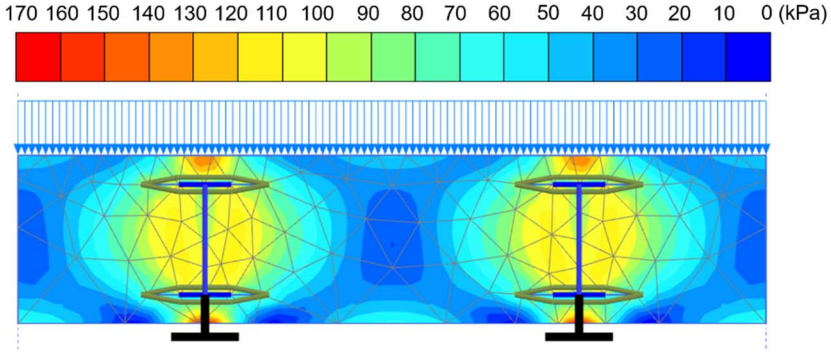

Fig. 8. Deviatoric stress, q, developing in the pressure arch (with $f_{sm,tk}$ = 0.1 MPa)

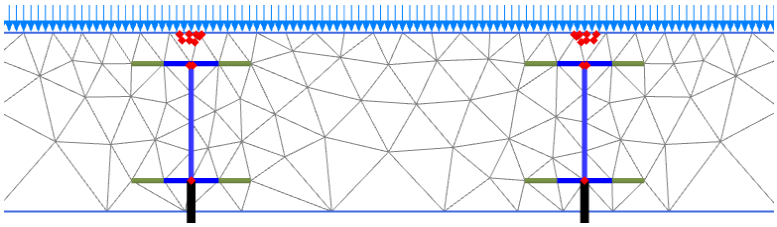

Fig. 9. Plastic points in the soil mix (red points = tension cut-off points) (FEM with $f_{sm,tk}$ = 0.1 MPa)

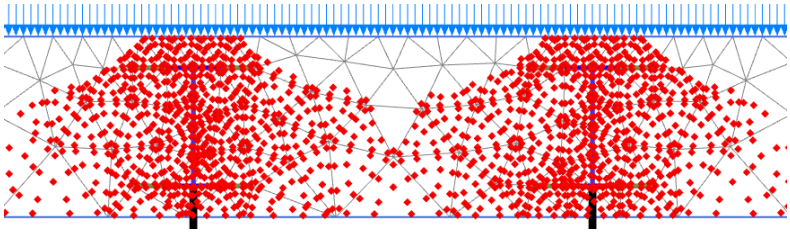

Fig. 10. Plastic points in the soil mix (red points = tension cut-off points) (FEM with $f_{sm,tk}$ = 0 MPa)

In order to investigate the **influence of the lateral boundaries**, an extended model with three simulated pressure arches has been implemented (see Fig. 11). The analysis is based on the comparison of the compressive and shear stress distributions computed along the same cross-sections than for the first simulations (Fig. 4, 5 and 6) but in the three different arches. As the stress values are the same in the three pressure arches, there is no boundary effect and the development of the stresses in the pressure arch can be studied with a model simulating only one pressure arch.

To study the **effect of the mesh** on the numerical results, a fine mesh is finally used. Moreover, in areas where large stress concentration or large deformation gradients are expected, local refinements (mesh density multiplied by 5) are applied. The densification and the local refinement of the mesh do not lead to different compressive and shear stress values than those obtained with the medium mesh. The medium mesh is thus suitable for such numerical analysis.

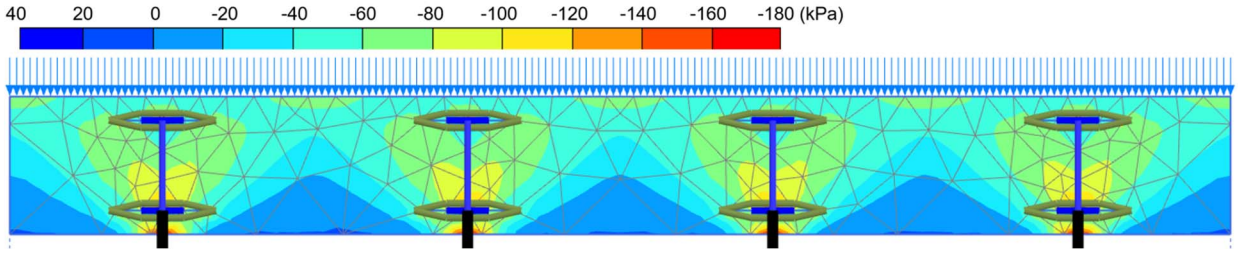

Fig. 11. Symmetry of the principal total stress σ_1 in the three pressure arches (with $f_{sm,tk}$ = 0.1 MPa)

VERIFICATION OF THE ARCHING EFFECT ACCORDING TO THE HANDBOOK

In practice, the geotechnical engineer responsible of the design of the soil mix walls generally uses analytical methods, as proposed in the handbook, to check the arching effect (see Fig. 2) according to the Eurocodes. In the present case, a temporary CSM panel reinforced with IPE 360 is considered with the properties given in Table 1. Temporary means that the lifetime of the wall is less than 2 years.

Before the verification of the pressure arch, it is still necessary to **determine the UCS design value** of the soil mix material, noted $f_{sm,d}$. According to the definitions of the handbook, $f_{sm,d}$, is determined as:

$$f_{sm,d} = \alpha_{sm} \frac{f_{sm,k}}{\gamma_{sm} k_f} \beta \qquad [1]$$

where, α_{sm}, the long-term factor is equal to 1 [-] for temporary and 0.85 [-] for permanent walls. γ_{sm} is the material factor equal to 1.5 in Belgium. k_f is a factor taking into account the way the UCS is determined: if the UCS is determined based on samples from the in situ walls, k_f is equal to 1.0 [-]; in all other cases, e.g. starting from 'estimated' values, this factor is equal to 1.1 [-]. β is a correction factor [-] for the young age of the soil mix material; depending on various factors, $\beta = 0.3$ to 0.7 after 7 hardening days and $\beta = 0.6$ to 0.8 after 14 hardening days. β is used in case of excavation a few days after the execution of the soil mix. In the present case, we consider the following values for these parameters: $\alpha_{sm} = \beta = 1$ [-], $\gamma_{sm} = 1.5$ [-] and $k_f = 1.1$ [-]. In the present case, $f_{sm,d}$ is therefore equal to 1.21 [MPa].

Considering the analytical methods proposed in the handbook, it must be first verified that the earth and water pressures can be transmitted to the steel beams via a pressure arch. According to Eurocode 2, EC2 (EN 1992-1-1), to ensure the arching effect, the **distance between the steel beams** must be limited:

$$l_s < 3H \qquad [2]$$

where l_s is the axis-to-axis distance between the steel beams and H the maximal height available for the development of the arch in the soil mix material (see Fig. 2): $H = h_a - t_f + \min(c_1;c_2)$. Considering the data of Table 1, that results in: 1.22 [m] < 1.33 [m]. The arching effect is thus verified according to EC 2.

After this first verification, the **geometry of the pressure arch** is broached with the determination of:
- the height of the pressure arch (noted z in Fig. 2),
- the angle α at the location of the base of the pressure arch (illustrated in Fig. 2),
- the thickness of the pressure arch at location of the beam, d_{bg}, and in the middle of the arch, $d_{bg;mid}$.

This determination is made by means of an iterative calculation varying α by assuming a parabolic function for the central line of the arch, i.e. the red line in Fig. 2.
The height of the arch is determined in agreement with the Dutch National Annex of EC2:

$$z_{bg} = 0.2\, l_s + 0.4\, H \leq 0.6\, l_s \qquad [3]$$

Moreover, for geometrical reasons:

$$z_{bg} \leq H - \frac{d_{bg;mid}}{3} \qquad [4]$$

where $d_{bg;mid}$ is the thickness of the pressure arch in the middle of the arch (cross-section) which is approximated by: $d_{bg;mid} = b_f \tan \alpha$ based on numerical analysis of the development of the pressure arch in the soil mix material. The factor 3 in equation [4] results from the apparent quasi-linear course of the compressive stress in the middle cross-section. In the present case, varying α, the verification is finally obtained for the following values: $\alpha = 50.7°$, $d_{bg;mid} = 208$ [mm], $z_{bg} = 373$ [mm]. In addition, the thickness of the pressure arch at the location of the beam can be assessed based on the angle α and considering the flange width of the beam b_f: $d_{bg} = b_f \sin \alpha = 132$ [mm].

The next stage is the **computation of the stresses developing in the soil mix arch**. This verification is based on a 'strut and tie' model given in Fig. 12.

The maximum compressive stress at the connection with the beam is first regarded. As demonstrated in the FEM calculations, the stress distribution at the location of the base of the beam is equally divided (see Fig. 13 for the sake of illustration). Therefore, the maximum compressive stress can be determined based on a calculated normal force (N'_{base}) and the established thickness of the arch (d_{bg}). A part of the

pressure applying on the wall is directly absorbed by the outer flange of the steel beam. The remaining part between the beams is transferred via the pressure arch. If one assumes that loads below 45º can be transferred to the outer flange, the design value (in Ultimate Limit States - ULS) of the load borne by the pressure arch is:

$$F_{hor;pressure\ arch} = F_{hor;tot} - F_{hor;outer\ flange} = \sigma_{hor}(l_s - b_f - 2c_1) = 43.0 \text{ [N/mm]} \quad [5]$$

with σ_{hor} the design value of the earth and water pressure (σ_{hor} is equal to 50 kPa in the present case study).

Considering the value of the angle α between the pressure arch and the flange beam (50.7°), the occurring normal force at the base of the flange is:

$$N'_{base} = \frac{0.5\ F_{hor;pressure\ arch}}{\sin\alpha} = \frac{0.5\ \sigma_{hor}(l_s - b_f - 2c_1)}{\sin\alpha} = 27.8 \text{ [N/mm]} \quad [6]$$

As a result, the compressive stress developing in the pressure arch is equal to:

$$\sigma'_{arch,base} = \frac{N'_{base}}{d_{bg}} = \frac{0.5\ \sigma_{hor}(l_s - b_f - 2c_1)}{(b_f \sin^2\alpha)} = 0.211 \text{ [MPa]} \quad [7]$$

The width of the horizontal beam of the strut and tie model of the Fig. 12 is noted l_{mid} and is computed as:

$$l_{mid} = l_s - 2\frac{z_{bg}}{\tan\alpha} = l_s - 2\frac{z_{bg}}{\left(\frac{4z_{bg}}{l_s}\right)} = \frac{1}{2}\ l_s = 0.61 \text{ [m]} \quad [8]$$

The <u>maximum shear force in the pressure arch</u> is found at the bend in the strut and tie model (see Fig. 12):

$$V_{mid} = 0.5\ l_{mid}\sigma_{hor} = 0.25\ l_s\sigma_{hor} = 15.25 \text{ [N/mm]} \quad [9]$$

Considering the shear stress distribution (illustrated in Fig. 14), the design value of the maximum shear stress is given by:

$$\tau_{Ed} = \frac{3}{2}\frac{V_{mid}}{d_{bg;mid}} = 0.110 \text{ [MPa]} \quad [10]$$

Finally, the <u>maximum compressive stress in the center of the pressure arch</u> is regarded. Contrarily to the base of the arch, FEM results show that a substantially linear stress distribution is formed in the center (cross-section) of the pressure arch (see Fig. 15). This is calculated on the assumption that the soil mix material cannot absorb any tension. Considering the geometry of the pressure arch in the strut and tie model and the Pythagorean theorem, the resultant normal force in the horizontal beam, N'_{middle}, is given by:

$$N'_{middle} = \sqrt{N'^2_{base} - V^2_{mid}} = 23.2 \text{ [N/mm]} \quad [11]$$

The average compressive stress in the middle of the arch $\sigma'_{arch;mid;avg}$ is then computed as $N'_{middle}/d_{bg;mid} = 0.112$ [MPa]. Nevertheless, the stress in the middle of the arch is not uniform (see Fig. 15). Assuming that the maximum absorbable tensile stress is reached (which is set equal to 0), on the tensile side, the normal compressive stress resulting of N'_{middle} is completely counterbalanced by the moment. At the compressive side, the compressive stress is then doubled:

$$\sigma'_{arch;mid;max} = 2\ \sigma'_{arch;mid;avg} = 0.223 \text{ [MPa]} \quad [12]$$

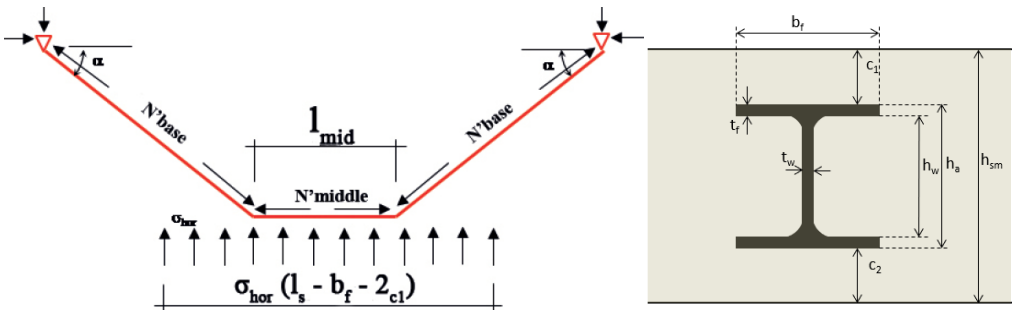

Fig. 12. Model for the verification of the arching effect in the soil mix (left) and notations (right)

Fig. 13. FEM: total normal stress distribution at the base of the pressure arch (with $f_{sm,tk}$ = 0 MPa)

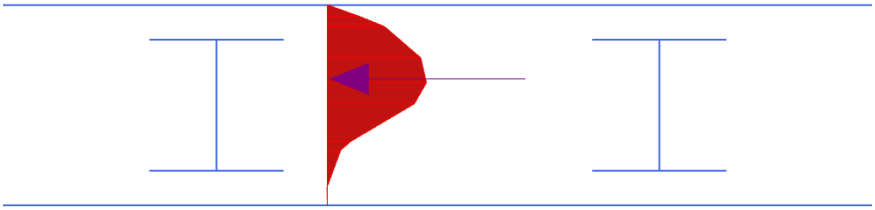

Fig. 14. FEM results: shear stress distribution along the cross-section corresponding to the bend in the strut and tie model, i.e. at $l_s/4$ (with $f_{sm,tk}$ = 0 MPa)

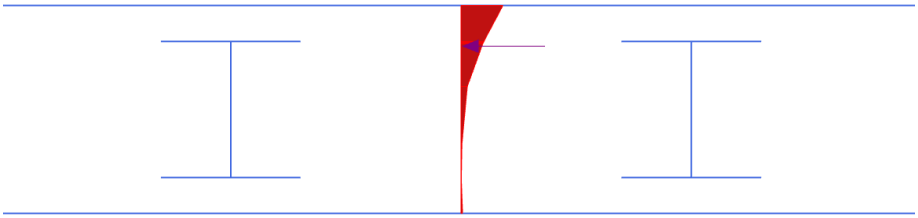

Fig. 15. FEM: total normal stress distribution in the middle of the pressure arch (with $f_{sm,tk}$ = 0 MPa)

Once the compressive and shear stresses arising in the pressure arch are determined, these values must be compared with the **admissible stresses** computed taking into account the resistance of the soil mix material. Distinction is made between the admissible compressive stress in the middle cross-section of the arch (considered as a compressive strut with transverse tension) and the admissible compressive stress at the base of the arch (considered as a connecting node). In the compressive strut, based on the condition that there is a compressive beam with tensile stress in the opposite direction, the design value of the admissible compressive stress in the center of the pressure arch is determined, according to EC2, by:

$$\sigma_{Rd,max,strut} = 0.6\,\nu'\,f_{sm,d} = 0.6\left(1 - \frac{f_{sm,k}}{250}\right) f_{sm,d} = 0.721\ [\text{MPa}] \qquad [13]$$

For the connection node, tensile stresses may occur in the vertical direction if the flange of the beam lies within the tensile zone. In consequence, according to EC2, the design value of the admissible compressive stresses at the node is given by:

$$\sigma_{Rd,max,node} = k_2\, \nu' f_{sm,d} = 0.85\left(1 - \frac{f_{sm,k}}{250}\right) f_{sm,d} = 1.022 \text{ [MPa]} \quad [14]$$

The admissible shear stress in the pressure arch is equal to the design value of the shear strength $\tau_{Rsm,d}$ which can be increased by 15% of the compressive stress in the pressure arch:

$$\tau_{Rsm,d} = f_{sm,td} + \frac{15}{100}\sigma'_{arch,mid,av} = \alpha_{sm}\frac{0.21 f_{sm,k}^{2/3}}{\gamma_{sm} k_f}\beta + \frac{15}{100}\sigma'_{arch,mid,av} = 0.219 \text{ [MPa]} \quad [15]$$

where $f_{sm,td}$ is the design value of the tensile strength of the soil mix material. According to EC2, in order to increase the shear strength with a proportion of the compressive stress developing in the pressure arch, $\sigma'_{arch,mid,av}$ (0.112 MPa) must be smaller than 0.2 $f_{sm,d}$ (0.242 MPa).

In the present case, the verification of the internal stresses arising in the pressure arch is established:
$\sigma'_{arch,base}$ = 0.211 [MPa] (equation 7) < $\sigma_{Rd,max,node}$ = 1.022 [MPa] (equation 14)
$\sigma'_{arch;mid;max}$ = 0.223 [MPa] (equation 12) < $\sigma_{Rd,max,strut}$ = 0.721 [MPa] (equation 13)
τ_{Ed} = 0.110 [MPa] (equation 10) < $\tau_{Rsm,d}$ = 0.219 [MPa] (equation 15)

COMPARISON OF THE FEM RESULTS WITH THE ANALYTICAL RESULTS OF THE HANDBOOK METHODOLOGY FOR THE VERIFICATION OF THE PRESSURE ARCH

In the present case, the finite element model with one simulated arch is used for the comparison which is made considering two tensile strengths for the soil mix material in the simulations: 0.1 and 0 MPa. It is to note that the value of the tensile strength of the soil mix material is not directly used in the analytical verification according to the handbook. The value of the tensile strength introduced in equation [15] is determined based on the characteristic UCS value of the soil mix material, $f_{sm,k}$. Table 3 provides the comparison between the FEM and the analytical results for the compressive and shear stresses arising in the pressure arch resulting from the application of a uniform pressure of 50 kPa on the wall. For the computation of the maximal stresses, cross-sections are selected in the numerical models in such a way that they correspond to the cross-sections considered in the analytical method. The calculated stresses are also compared with the resistance of the soil mix material computed considering the design approach of the handbook. Analytical stress values are computed considering: $\alpha_{sm} = \beta = k_f = \gamma_{sm} = 1$ [-] as the characteristic values are used for the realization of the numerical simulations.

Table 3. FEM and analytical results for the stresses developing inside the pressure arch generated by the application of a uniform pressure of 50 kPa on the wall

	FEM results with $f_{sm,tk}$ = 0.1 MPa [kPa]	FEM results with $f_{sm,tk}$ = 0 MPa [kPa]	Handbook - analytical results [kPa]	Handbook - resistance [kPa]
Maximal† compressive stress at the base of the pressure arch, $\sigma'_{arch,base}$ (kPa)	between 117 and 125 if α is slightly varied‡	between 190 and 240 if α is slightly varied‡	211 See equation [7]	1686
Maximal† compressive stress in the middle of the pressure arch, $\sigma'_{arch;mid;max}$ (kPa)	79 (see Fig. 5 for the selected cross-section)	222 (see Fig. 15 for the selected cross-section)	223 See equation [12]	1190
Maximal† shear stress in the pressure arch, τ_{Ed} (kPa)	64♣ and 40‖	110♣ and 55‖	110 See equation [10]	350

†Maximal stress value for the stress distribution developing along the determined cross-section
‡for the determination of $\sigma'_{arch,base}$, the angle α deduced from the analytical approach is initially used. Afterwards, an extra analysis is conducted varying the value of α to observe the effect of this variation on the value of $\sigma'_{arch,base}$: see Fig. 4 and 13 for the selected cross-sections
‖along a cross-section corresponding to the bend in the strut and tie model, i.e. at $l_s/4$: see Fig. 14 for the selected cross-section
♣ along a cross-section at the boundaries of the flanges of the steel beam: see Fig. 6 for the selected cross-section

The numerical values of the stresses obtained when a tensile strength of 0.1 MPa is taken for the soil mix material are smaller than the analytical values. A relatively good correspondence is observed between the numerical and the analytical results when a tensile strength of 0 MPa is used in the numerical simulations what is logical considering the assumptions made in the development of the analytical method regarding the compressive and shear stress distributions. As aforementioned, the maximal stress values obtained from the numerical simulations are dependent on the cross-section selected for the stress analysis. These values can therefore vary in function of the selected cross-section.

SUMMARY AND CONCLUSIONS

In the present article, 2D finite element simulations, conducted with PLAXIS, are used in order to study the arching effect arising in soil mix panels when subjected to the pressure acting behind the retaining wall. The effect of the tensile resistance of the soil mix material is first investigated. When this tensile resistance is decreased, the stress pattern in the soil mix material evolves and the arching effect is accentuated. If no global failure or instability of the CSM panel is observed for a uniform pressure of 50 kPa applied on the wall, the decrease of $f_{sm,tk}$ to 0.1 MPa and then until 0 leads to the emergence of plastic points in the material where the tensile strength of the soil mix material is reached.

With $f_{sm,tk}$ = 0 MPa, the maximum compression stress, observed in the middle of the arch, is almost doubled in comparison with the compression stresses obtained with $f_{sm,tk}$ = 2 or 0.1 MPa. No effect of the model boundaries or of the mesh refinement on the numerical results has been observed for the present configuration of the CSM panel.

The results of the simulations were compared with results of analytical computations realized according to the methodology proposed in the BBRI/SBRCURnet Handbook – Soil mix walls (2018) and that for two tensile strengths considered in the FEM for the soil mix material: 0 and 0.1 MPa. The numerical values of the stresses, obtained when a tensile strength of 0.1 MPa is considered, are smaller than the analytical values. A relatively good correspondence is observed between the numerical and the analytical results when a tensile strength of 0 MPa is used in the numerical simulations what is logical considering the assumptions of the analytical method. As aforementioned, the maximal stress values obtained from the numerical simulations are dependent on the cross-section selected for the stress analysis. These values can therefore vary in function of the selected cross-section. With FEM software used for the verification of the arching effect developing in the CSM panel, it will be therefore important to consider an approach based on the internal resultant forces in addition to the analysis of local stress distributions.

ACKNOWLEDGMENTS

This work was supported by the CWALity DE research program of the Walloon Region (Direction des Programmes de Recherche). This support is gratefully acknowledged.

REFERENCES

BBRI/SBRCURnet. 2018. Handbook Soil mix walls. Taylor and Francis Group, ISBN 978 90 5367 641 7.

EN 1992-1-1: 2004. Eurocode 2: Design of concrete structures.